Published in final edited form as:
Osteoarthritis Cartilage. 2008 August ; 16(8): 909–918. doi:10.1016/j.joca.2007.12.003.

Static and dynamic compressive strains influence nitric oxide production and chondrocyte bioactivity when encapsulated in PEG hydrogels of different crosslinking densities

I Villanueva, M.S.[†], **DS Hauschulz**[†]**[Electromechanical Engineer]**, **D Mejic**[†]**[Instrument Maker]**, and **SJ Bryant, PhD**[*,†]**[Assistant Professor]**

[†]Department of Chemical Engineering, University of Colorado, Campus Box 424, Engineering Center, ECCH 111, Boulder, CO 80309-0424, USA

Summary

Objective—Mechanical loading is an important regulator of chondrocytes; however, many of the mechanisms involved in chondrocyte mechanotransduction still remain unclear. Here, poly(ethylene glycol) (PEG) hydrogels are proposed as a model system to elucidate chondrocyte response due to cell deformation, which is controlled by gel crosslinking (ρ_x).

Methods—Bovine articular chondrocytes (50×10^6cells/ml) were encapsulated in gels with three ρ_x's and subjected to static (15% strain) or dynamic (0.3Hz or 1Hz, 15% amplitude strain) loading for 48 hours. Cell deformation was examined by confocal microscopy. Cell response was assessed by total nitric oxide production (NO), proteoglycan (PG) synthesis ($^{35}SO_4^{2-}$-incorporation) and cell proliferation ([^{3}H]-thymidine incorporation) (CP). Oxygen consumption was assessed using an oxygen biosensor.

Results—An increase in ρ_x led to lower water contents, higher compressive moduli, and higher cell deformations. Chondrocyte response was dependent on both loading regime and ρ_x. For example, under a static strain, NO was not affected, while CP and PG synthesis were inhibited in low ρ_x and stimulated in high ρ_x. Dynamic loading resulted in either no effect or an inhibitory effect on NO, CP, and PG synthesis. Overall, our results showed correlations between NO and CP and/or PG synthesis under static and dynamic (0.3 Hz) loading. This finding was attributed to the hypoxic environment that resulted from the high cell-seeding density.

Conclusion—This study demonstrates gel ρ_x and loading condition influence NO, CP, and PG synthesis. Under a hypoxic environment and certain loading conditions, NO appears to have a positive effect on chondrocyte bioactivity.

Keywords

chondrocyte; hydrogels; poly(ethylene glycol); cell deformation; mechanical loading; nitric oxide; hypoxia

[*]Corresponding author: Department of Chemical and Biological Engineering, UCB 424 ECCH 111, Boulder, CO, 80309, USA. Tel: (303) 735-6714; Fax: (303) 492-4341; stephanie.bryant@colorado.edu.

Introduction

The structure of the ECM and its components are essential for articular cartilage to function properly under normal physiological loads. The ECM is maintained by a balance between anabolic and catabolic activities of the resident chondrocytes in which mechanical forces play a key role. During normal physiological activities, articular cartilage is continuously subjected to stresses that induce strain related deformations in the tissue causing, for example, deformation in the cell membrane, fluid flow, streaming potentials, and hydrostatic pressures[1–4]. These extracellular events are sensed by the chondrocytes to initiate a cascade of intracellular signaling events that ultimately influence cell metabolism. This process is termed mechanotransduction. However, many of the mechanisms involved in mechanotransduction remain unresolved.

It is well known that when a joint is under or overloaded, mechanotransduction pathways in chondrocytes are altered leading to adverse changes in the cartilage ECM structure. Over time, these abnormal structural changes in the tissue can lead to impaired joint motion, excessive pain and eventually osteoarthritis (OA)[5,6].

Nitric oxide (NO) is an inter- and intracellular signaling molecule in chondrocytes[7], which has been implicated as a mediator of OA[5]. NO, when stimulated by inflammatory cytokines, has been shown to enhance catabolic activities by chondrocytes and lead to cartilage degradation[9–12]. For example, NO has been shown to suppress proteoglycan synthesis[13], stimulate the production of matrix metalloproteinases[14], and promote cell cycle arrest[15–17]. Under hypoxic culture conditions, however, NO has been reported to have a protective role in chondrocytes by promoting anabolic activity, e.g. proteoglycan synthesis, in the absence of inflammatory cytokines[18,19].

Several 2D and 3D models have been used to examine the role of NO in chondrocyte mechanotransduction[2,20–25]. For example, fluid induced shear stress resulted in increased NO production by chondrocytes cultured in monolayer, which was correlated to an increase in proteoglycan synthesis[20]. When cartilage explants were subjected to either static compressive strains for 24 hours at 0.1 MPa or intermittent compressive strains of 0.5–1 MPa at 0.5 Hz for 6 hours, increases in NO production were observed[26]. To isolate the inter-related processes that occur during mechanical loading in native cartilage, several investigators have utilized chondrocytes seeded in agarose as a model system to study pathways involved in cell deformation[22,27,28,29]. In this model system, chondrocytes deform to the same degree as the strain applied to the agarose construct[28]. When agarose constructs were subjected to mechanical loading during early culture times, dynamic loading inhibited nitric oxide production and stimulated cell proliferation and proteoglycan synthesis while static loading caused an opposite response[30]. Decreases in NO production were correlated with increases in cell proliferation suggesting that cell deformation may play a role in mechanotransduction pathways that involve NO and cell proliferation[30].

Recently, three dimensional crosslinked PEG hydrogels have been proposed as an alternate model to study chondrocyte deformation and cell response to mechanical loading[31,32]. An attractive feature of PEG gels is the fact that their properties are readily controlled with high fidelity. For example, PEG gels can be tailored to exhibit properties similar to native cartilage without compromising cell viability or function[33]. When a gross compressive strain was applied to cell seeded PEG hydrogels, the degree of cell deformation was dependent on the crosslinking density. Therefore, PEG hydrogels provide two levels of control over cell deformation through the applied strain and the crosslinking density. When chondrocyte seeded PEG constructs were subjected to dynamic loading at a frequency of 1 Hz during early culture times, cell proliferation and proteoglycan synthesis were inhibited and this

inhibition was further enhanced with increased crosslinking density. This study, however, was limited to examining one loading frequency (1Hz).

In the current study, PEG hydrogels were used to examine differences in chondrocyte response under a broader range of gel crosslinking densities and loading conditions (static loading at 15% compressive strain and dynamic loading at 0.3 Hz or 1 Hz with 15% amplitude strains). Chondrocyte response was measured as a function of total nitric oxide production, cell proliferation and proteoglycan synthesis. To elucidate the role of NO in chondrocyte mechanotransduction, correlations between nitric oxide and cell proliferation or proteoglycan synthesis were assessed. This information will not only provide insights into chondrocyte mechanotransduction but may also elucidate suitable loading conditions and hydrogel structures for cartilage regeneration.

Materials and Methods

Chondrocyte Isolation

Full depth articular cartilage was removed under sterile conditions from the metacarpalphalangeal joints of front feet from five different adult steers (2–4 years) within several hours after slaughter and washed in phosphate buffered saline (PBS, Invitrogen, California, USA). The cartilage slices were washed in PBS supplemented with 1% penicillin-streptomycin (PBS-P/S, Invitrogen, California, USA), diced finely and incubated at 37°C for a maximum of 16 hours in 0.2% collagenase type II (Worthington Biochemical Corp, New Jersey, USA) in Dulbecco's Minimal Essential Medium (DMEM, Invitrogen, California, USA) supplemented with 20% fetal bovine serum (FBS, Invitrogen, California, USA). The suspended chondrocytes were centrifuged three times at 1200 rpm for 10 minutes, and resuspended in PBS-P/S. Cell viability was greater than 96% prior to encapsulation as determined by trypan-blue exclusion test.

Polymer Preparation

Poly(ethylene glycol) (PEG) (3000 MW, Fluka, USA) was dissolved in methylene chloride and reacted with excess methacryloyl chloride and triethylamine under argon for 24 h at 4°C. The reaction by-products were removed by filtration and precipitation in acetone. The final product, poly(ethylene glycol) dimethacrylate (PEGDM) was precipitated twice in cold ethyl ether and vacuum filtered to remove remaining impurities. The degree of methacrylate substitution was 80% as determined by ^{1}H NMR (Varian VYR-500, California, USA). Specifically, the area under the integral for the vinyl resonances (δ=5.6ppm and δ=6.2 ppm) associated with the methacrylate substitution was compared to that of the methylene protons (δ=4.3ppm) on the PEG backbone.

Chondrocyte Encapsulation

Hydrogels were fabricated from a solution of PEGDM macromer and photoinitiator (1-[4-(2-hydroxyethoxy)-phenyl]-2-hydroxy-2-methyl-1-propane-1-one) in PBS (pH 7.4) or deionized-H_2O. PEGDM concentrations were varied from 10, 20, to 30% (w/w) with photoinitiator concentrations of 0.05, 0.0125, and 0.0056% (w/w), respectively. Isolated chondrocytes were suspended in the macromer/initiator solution at a concentration of 50×10^6 cells/mL and exposed to 365 nm light at ~2 mW/cm^2 for 10 min to entrap the cells within cylindrical PEG hydrogels (5mm in diameter and 5mm in height). Cell-laden hydrogel constructs were cultured under free swelling conditions in individual wells of a 24 well tissue culture plates containing 1.5 mL per well of chondrocyte media (10mM HEPES, 0.1M non-Essential Amino Acids, 0.4 mM L-proline, 50mg/L L-ascorbic acid, 1% P/S, 10% FBS, and 0.5μg/mL fungizone (all from Invitrogen Corp, California, USA) in DMEM) for 24 hours prior to the application of loading.

Hydrogel Properties

Cylindrical PEG hydrogels (5 mm in height and 5 mm in diameter) without cells were swollen to equilibrium for 24 h in a PBS buffer solution at 37°C. The swollen mass of the gel was measured. The gel was lyophilized for 24 h to determine the dry polymer mass. Equilibrium volumetric swelling ratio (Q) was determined from the equilibrium mass swelling ratio as described previously[32]. The gel crosslinking density, ρ_x, was estimated from the equilibrium swelling data using a modified version of the Flory–Rehner equation neglecting chain ends[34]. The tangent compressive modulus was determined using a mechanical tester (MTS Synergie 100, Minnesota, USA) in unconfined compression equipped with nonporous platens. A constant strain rate of 0.02 mm/s was applied to the hydrogels and the resulting stress was recorded. The dynamic modulus was measured in unconfined compression (Bose Force Testbench System, Minnesota, USA) under conditions mimicking the bioreactor. An offset strain (corresponding to the strain from the weight of the pins) was applied to the gel followed by the application of a cyclic compressive strain from 0 to 15% strain in a sinusoidal waveform at a frequency of 0.3Hz or 1.0Hz. The resulting stress was recorded as a function of time. The mechanical properties were measured under hydrated conditions. A sample size of 5–6 was used.

Mechanical Loading

A custom mechanical loading apparatus (Figure 1) was built based on a previous design by Lee *et al.*[22]. In our system, a unique drive mechanism was developed, which consists of a stepper motor connected to a loading platform via a crank and compound linkage assembly. The loading platform can be precisely lifted and lowered to compress the hydrogel samples with a minimum of load reflected back to the motor. The mechanism operates near its full extended (upright) position to confer both mechanical advantage and maximum resolution of platform displacement. In a sense, the rod and motor linkages act like a gearless gear reducer. In this application a relatively large lateral displacement applied with a low force to the joint rod was transformed into a small vertical displacement of high force to the loading platform. Because there are no gears, the motion is very smooth and free from backlash that can often plague gear systems.

The crank radius was sized to require the stepper motor (Applied Motion Systems, Washington, USA) to sweep the better part of the full rotation to maximize the ratio of motor steps to the magnitude of sample compression. Our stepper motor has 200 full steps/revolution. This motor is driven by an electronic Gecko G212 motor driver (GeckoDrive, California, USA) and Galil DMC-1417 (Galil Motion Products,USA) motion control card configured to drive at 20000 microsteps/revolution. One full revolution of the motor produces 1.78 mm of compression at the sample. Thus, the compound mechanism can resolve 1 micro step out of 20,000 which translates to 1/20,000 × 1.78 mm = 0.09 microns. Practical experience in the lab indicates a repeatable accuracy of +/− 1 micron. Therefore, this device realizes 0.1% full stroke accuracy when a sample is compressed 1 mm. In addition to micro-stepping, the Galil DMC-1417 controller card can be programmed to control waveform, strain and frequency. A Schaevitz LVDT HR 200 linear voltage displacement transformer (MSI Sensors, Virginia, USA) is connected to the loading platform to verify movement distance.

A standard 24-well plate fits into the apparatus and each well was associated with a loading pin. The platens of each loading pin were fabricated from non-porous Delrin®. Each loading pin weighs approximately 5 grams. The platform contains an outer acrylic casing (Figure 1) that ensures sterile culture conditions once placed inside an incubator (Heraeus Instruments, USA) at 37°C and 5% CO_2.

After free swelling for 24 hours, constructs were placed into the loading apparatus with 1.5 mL of chondrocyte media containing 1μCi/mL of [^{3}H] thymidine and 10μCi/mL of [$^{35}SO_4^{2-}$] (Perkin Elmer, Connecticut, USA) per well. The inner 12 pins are locked to the horizontal platform serving as the loaded specimen, while the remaining outer 12 pins remain free and served as the unstrained controls. The hydrogel constructs were subjected to one of three loading regimens for 48 hours: (i) static 15% compressive strain, (ii) 0.3 Hz at 15% amplitude strains (actual controller frequency was 0.33 Hz), and (iii) 1 Hz at 15% amplitude strains (actual controller frequency was 0.98 Hz). The percent strain was based on the initial heights of the gel constructs, but the height of the gel did not change over the course of the experiment. The weight of the pins imparts an initial strain to the gels, which is dependent on the gel compressive modulus. The offset strains were 4.8, 0.7 and 0.5% for the low, medium and high crosslinked gels, respectively.

Chondrocyte Viability

Immediately post loading, cell viability was semi-quantified in two separate gels, using a membrane integrity assay, LIVE/DEAD® (Invitrogen, California, USA), in which live cells fluoresce green and dead cells fluoresce red. Images (225μm × 225μm) were obtained using a laser scanning confocal microscope (Zeiss LSM 5 Pascal) equipped with a 10X water immersion objective. Each cylindrical gel was cut into 3 equal horizontal sections representing the top, middle and bottom. A total of 2 images were taken approximately 200 microns into the gel from each section. Cell viability was quantified manually by counting live and dead cells in each image.

Chondrocyte Deformation

Gel constructs were placed in a custom designed cell strainer apparatus similar to that described by *Knight et.al.*[28]. The cell strainer sits on the stage of inverted microscope associated with a confocal laser scanning unit. Images were obtained for each cell at full width half maximum height under no strain and under an applied static strain. A total of 3 images at different focal planes with an overall average cell count of 48 cells were recorded for each gel. A total number of 2 gels per gel formulation were used for an n=96 for each experimental condition. Cell morphology was measured as a diameter ratio (x/y) in which × is the cell diameter parallel to the applied strain and y is the cell diameter perpendicular to the applied strain[22,27–28].

Biochemical Assays

After 48 hours of loading, the culture medium was removed from each well and stored at −20°C until further analysis. A total of eight constructs per condition were removed from the loading apparatuses and crushed using a tissue homogenizer followed by enzymatic digestion (125μg/mL of papain (Worthington Biochemical, New Jersey, USA), 10mM of L-cysteine-HCl (Sigma, Missouri, USA), 100mM of phosphate (Sigma, Missouri, USA) and 10mM of EDTA (Biorad, California, USA) at a pH of 6.3 for 16 hours at 60°C. Hoeschst 33258 (Polysciences, Pennsylvania, USA) fluorescence assay was used to quantify total DNA content in the papain digest[35].

The amount of $^{35}SO_4^{2-}$ incorporation into newly synthesized proteoglycans (PGs) was determined in the papain digests using the Alcian blue precipitation method[22,36,37]. [^{3}H]-Thymidine incorporation into newly synthesized DNA was measured in the papain digests by 10% (w/v) trichloroacetic acid precipitation. Both $^{35}SO_4^{2-}$ and [^{3}H] from the digests were placed onto filters using the Millipore Multiscreen system (Millipore, Maryland, USA)[22]. Nitrate and nitrite were measured in the media using the Colorimetric Total Nitric Oxide Assay Kit (Cayman Chemicals, Michigan, USA) to determine the total nitric oxide (NO) production.

Oxygen consumption

Gel constructs were photopolymerized (as described above) directly in wells of a 96-well oxygen biosensor plate (BD Biosciences, California, USA). The height of the gel was 2.5mm, which represents half of the thickness of the constructs used in this study and therefore corresponds to the center of the construct. Chondrocyte media (200μL) was added to each well immediately after polymerization and incubated at 37°C and 5% CO_2. Oxygen concentration was measured at the base of the well at 0 and 48 hours using a fluorometer (BMG Labtech Fluostar Optima, North Carolina, USA). Oxygen consumption was calculated at the base of the well using the Stern-Volmer equation described elsewhere[38].

Statistical Analysis

Single factor ANOVA was performed to examine differences in nitric oxide, cell proliferation and PG synthesis in gels that were strained versus unstrained as a function of gel crosslinking and loading condition. The data in Tables 1,2, and 6 are presented as the mean +/− standard deviation and the data in Table 3, Figure 3, and Figure 4 are presented as the mean +/− standard error of mean. Statistical analyses based on a single factor ANOVA are given in Table 4 for the static loading experiment. An ANOVA two factor fixed effects model was used to measure the interaction between gel crosslinking and dynamic loading (Table 5). A linear regression analysis was performed on the data for total NO production versus cell proliferation and on total NO production versus PG synthesis. In all analyses, a confidence level of 0.05 was considered statistically significant.

Results

Hydrogel macroscopic properties were controlled through initial changes in the PEGDM macromer concentration prior to polymerization (Table 1). Specifically, 10, 20 and 30% (w/w) PEGDM concentrations were used to create hydrogels in which the gel crosslinking density ranged from 0.110 to 0.650 mol/l. This increase in gel crosslinking resulted in a decrease in the volumetric equilibrium swelling ratio from 12.2 to 4.7 and an increase in the tangent compressive modulus from 60 kPa to 900 kPa. The dynamic modulus increased from 70 to 1200 kPa for gels subjected to 0.3 Hz and was overall higher in gels subjected to 1 Hz, increasing from 100 to 1400 kPa.

Bovine articular chondrocytes were photo-encapsulated in PEG hydrogels in each of the three crosslinking densities and cultured as unstrained controls or subjected to one of three loading regimens for 48 hours. Overall chondrocyte viability was above 70% and statistically similar for all gel compositions and culture conditions (strained or unstrained gels) (Table 2). In addition, no significant differences in cell viability were found as a function of depth within each hydrogel and each experimental condition. Representative micrographs of chondrocytes encapsulated in PEG hydrogels of each composition and either cultured as unstrained controls or subjected to 1 Hz dynamic loading conditions are shown in Figure 2. Similar images were obtained for gels cultured under static and 0.3 Hz loading conditions (data not shown). The micrographs also illustrate that chondrocytes were uniformly distributed throughout the construct.

To study cell morphology, cell diameters and diameter ratios were measured for each crosslinked gel after 72 hours of free swelling culture. Each gel composition was examined at 0% strain and under a static compressive strain mimicking the strains applied by the bioreactor (Table 3). Specifically, a 15% strain plus the offset strain associated with the weight of the pin was applied to each gel. Strains of 19.8, 15.7, and 15.5% were applied for the low, medium and high crosslinked gels, respectively. In the absence of strain, cell diameters were ~12 μm and the diameter ratios were approximately unity for each gel

crosslinking. Upon the application of a static strain, the cell diameter in the direction of the applied strain (x-diameter) decreased significantly while the cell diameter in the direction perpendicular to the applied strain (y-diameter) increased. For each gel crosslinking, the resulting diameter ratio decreased significantly upon the application of a static strain. In addition, diameter ratios decreased significantly with increases in the gel crosslinking (ANOVA, $p<0.05$).

Total NO production, cell proliferation and PG synthesis in gels subjected to static and dynamic loading were normalized to their respective unstrained control gels to isolate the effects of loading from the effects of gel crosslinking on cell response. The data are presented as a percent change from unstrained controls in Figures 3 and 4 for the static and dynamic loading experiments, respectively. Statistical analyses are presented in Tables 4 and 5 for the static and dynamic loading experiments, respectively.

Under an applied static strain, total nitric oxide production was statistically similar to the unstrained controls for each crosslinked gel and was not affected by changes in gel crosslinking. Cell proliferation was inhibited in the low and medium crosslinked gels, but stimulated in the high crosslinked gels by 83%. Proteoglycan synthesis was inhibited in gels with low crosslinking, but stimulated in gels with medium and high crosslinking by 91 and 29%, respectively.

When gel constructs were subjected to 0.3 Hz loading frequency, an increase in gel crosslinking density resulted in a significant decrease in total NO production (ANOVA, $p<0.05$) with an overall inhibition in PG synthesis, but no significant differences in cell proliferation. In the low crosslinked gel, an increase in loading frequency from 0.3 to 1 Hz resulted in an increase in total NO production, a decrease in cell proliferation, but no effect on PG synthesis. Similar trends were observed for the medium crosslinked gel, but PG synthesis was significantly reduced with higher loading frequency. In the high crosslinked gels an increase in loading frequencies did not have a significant effect on total NO production or cell proliferation, but resulted in a significant increase in PG synthesis. A significant interaction between gel crosslinking density and loading frequency led to varied responses in total NO production, cell proliferation and PG synthesis ($p<0.001$, $p<0.001$, $p<0.001$, respectively, Table 5).

Oxygen consumption was measured as a function of crosslinking density at a distance (2.5 mm) that represented the middle of the gel constructs. The data are presented in Table 6. Oxygen consumption decreased by 88% after 48 hours of free swelling culture. There were no significant differences in oxygen consumption as a function of gel crosslinking.

A simple linear regression statistical analysis was performed to determine if correlations exist between total NO production and cell proliferation or between total NO production and PG synthesis under mechanical loading (Figure 5). Under an applied static strain, there was a positive correlation between total NO production and cell proliferation ($R=0.5$; $p<0.05$) but no correlation was found between total NO production and PG synthesis ($R=0.1$; $p=0.67$). No significant correlations were found for the dynamic loading conditions. However, when examining each dynamic loading frequency separately, a positive correlation was found between NO and cell proliferation ($R=0.54$; $p<0.01$) and NO and PG synthesis ($R=0.73$; $p<0.01$) at 0.3Hz. No correlations between total NO production and cell proliferation or PG synthesis were found at 1 Hz.

Discussion

Neutral crosslinked PEG hydrogels of different crosslinking densities were fabricated as a 3D model system to study chondrocyte response due to changes cell deformation. When a

static strain is applied to PEG constructs of different crosslinking densities, an increase in the gel crosslinking leads to an increase in cell deformation. This result is due to the macroscopic heterogeneities that form in the network structure during polymerization where the degree of heterogeneity increases with higher crosslinking densities[31]. Here, three crosslinking densities were examined, which led to gels with a range of water contents and mechanical properties without sacrificing cell viability. For example, the high crosslinked gel imbibes 82% water, has a tangent compressive modulus of 900 kPa, and has a dynamic modulus in the range of 1200 to 1400 kPa depending on the loading frequency. In addition, the chemically crosslinked nature of the PEG gels results in little stress relaxation under a constant strain[31]. As a result, deformation of the encapsulated cells will closely follow the applied gross strain enabling efficient transfer of the applied strain from the construct to the cells during each cycle. For this study, an increase in the gel crosslinking density resulted in a significant increase in the degree of cell deformation even though the applied strain was highest in gels with lowest crosslinking (ANOVA, $p<0.05$).

When a gross static strain is applied to PEG hydrogels, a continuous strain is imparted on the encapsulated chondrocytes, which will be dependent on the crosslinking density. Interestingly, static loading did not influence total NO production. However, in the low crosslinked gels, static loading inhibited cell proliferation and PG synthesis. These results are in close agreement with studies performed on cartilage explants and agarose constructs[22, 26]. Interestingly, in gels with medium crosslinking, matrix production was significantly enhanced by static loading and to a lesser degree in the high crosslinked gels. One key difference between the low crosslinked gel and the medium or high crosslinked gel is the diffusional properties of newly synthesized matrix molecules[39]. The gel structure in the low crosslinked gels is sufficiently large to enable proteoglycan molecules to diffuse throughout the gel. In contrast, the structure of the medium and high crosslinked gels restricts matrix diffusion causing localization of newly synthesized matrix to remain in the pericellular region. Although limited matrix is produced during early culture times[31], localized proteoglycan molecules in the pericellular regions may lead to differences in the ionic and osmotic environment surrounding the cells which is further enhanced under static loading as fluid is expressed from the gel[40]. Quinn *et al*.[41] demonstrated that static loading applied to cartilage explants led to increased PG synthesis in the pericellular matrix, although overall PG synthesis decreased in the explant when compared to free swelling controls. Therefore, this difference in localization of PGs in the pericellular regions as a result of the gel crosslinked structure may provide additional outside-in signals to the entrapped cells to affect matrix production. Interestingly, cell proliferation was also enhanced in gels with high crosslinking densities under static load. It is possible that this pericellular environment may also influence pathways involved in cell proliferation. Further studies are necessary to elucidate the role of gel crosslinking on the pericellular environment and its affect on chondrocyte response.

Dynamic loading produces a much more complex environment involving both cell deformation and fluid flow, which will influence cell response within the PEG hydrogels. While the degree of cell deformation varies with crosslinking density, the total number of cycles, and therefore the total number of times the cells deform, will vary with frequency. In addition, induced fluid flow through the gels is likely to be dependent on a combination of factors including crosslinking density and frequency. The PEG crosslinks provide the structural support of the hydrogel similar to the crosslinks formed between the collagen fibers in native cartilage. Previous studies have shown through finite element modeling that the tissue modulus, which is a function of the collagen crosslinks, modulates fluid flow[42].

Interestingly, dynamic loading of PEG constructs had either no effect or an inhibitory effect on total NO production, cell proliferation, and proteoglycan synthesis at the frequencies

studied. Our results are contrary to published data from cartilage explants and agarose constructs at similar loading frequencies and strains in which dynamic loading for 48 hours enhanced matrix production[22,43]. For example, Sah *et al.*[43] demonstrated that in cartilage explants, dynamic loading frequencies between 0.01 to 1.0 Hz resulted in a 20 to 40% increase of proteoglycan synthesis compared to unstrained controls. Similarly, dynamic loading of chondrocyte seeded agarose constructs with frequencies ranging from 0.01 to 1.0 Hz resulted in enhanced PG synthesis from 6 to 13% during early culture from 2–5 days[44]. These differences in cell responses may be in part due to the structural differences in PEG compared to cartilage explants and agarose. For example, a 20% strain applied to crosslinked PEG hydrogels resulted in only a ~10% decrease in peak stress within 15 minutes owing to the predominantly elastic network[31]. On the other hand, cartilage and agarose exhibit large stress relaxation under load due to their viscoelastic properties. For example, a 10% strain applied to an agarose gel resulted in an 80% decrease in the peak stress within 15 minutes[45]. Therefore, the strains imparted on the chondrocytes will be significantly different when encapsulated in PEG compared to cartilage explants or agarose gels over the course of the experiment.

Our results from the dynamic loading studies generally demonstrate that an increase in gel crosslinking (corresponding to an increase in cell deformation) leads to decreases in total NO production and decreases and/or inhibition in cell proliferation and proteoglycan synthesis. In addition, an increase in the loading frequency generally led to higher total NO productions but lower cell proliferation and PG synthesis. However, there was one notable exception in the high crosslinked gels where an increase in loading frequency from 0.3 to 1 Hz resulted in increased PG synthesis. It is possible that changes in the cell environment (due to localization of newly synthesized molecules and/or higher cell deformations) led to this up-regulation in PG production.

Overall, our results indicate that a combination of cell deformation (through increases in gel crosslinking) and certain mechanical loading conditions (static and/or 0.3 Hz) lead to statistically significant positive correlations between total NO production and cell proliferation and between total NO production and PG synthesis. This finding is contrary to other model systems where opposite correlations were observed in which an increase in NO led to decreases matrix formation[9, 20,22,30,46–47] and cell proliferation[15,22,46,47]. However, previous studies have found that under low oxygen tension, endogenous NO has a cytoprotective role resulting in enhanced matrix production[48]. For example, monolayer articular chondrocytes cultured under hypoxic conditions resulted in an increase in hyaluronan synthesis[49]. Similar findings were observed when chondrocyte seeded porous poly(lactic acid) scaffolds were cultured under hypoxic (5% O_2) conditions, which led to increased PG production; however, cell proliferation was not affected[50]. We hypothesized that the high cell concentrations used in this study led to a hypoxic environment within the PEG hydrogels, and therefore in the absence of oxygen, total NO production exhibited a correlation with chondrocyte response. Here, we demonstrate that oxygen concentration decreased by 88% at the center of the construct for all three crosslinked gels. Although there will be an oxygen concentration gradient radially in the construct, this finding demonstrates that a significant portion of the hydrogel construct will be hypoxic. A similar reduction in oxygen tension was found when comparable cell concentrations were employed in agarose constructs[51]. It is possible that dynamic loading, in the case of 0.3 Hz, decreased total NO production and in the absence of oxygen led to decreased matrix production. Additional studies are necessary to elucidate the pathways involved.

In summary, we demonstrate that changes in gel crosslinking densities lead to changes in cell deformation. However, the combined effects of loading and gel crosslinking on chondrocyte response are likely to be more involved than simple changes in cell

deformation. Although PEG is a neutral hydrogel, early synthesis of extracellular matrix molecules may influence cellular responses due to an osmotic and/or ionic environment, which is likely to be dependent on the crosslinked structure. Nonetheless, we demonstrate an interesting finding in which a positive correlation was observed between NO and cell proliferation and between and NO and PG synthesis under certain mechanical loading conditions suggesting a potential pathway involved in chondrocyte mechanotransduction. The exact mechanisms of these pathways remain to be elucidated. Since cartilage is an avascular tissue, chondrocytes within cartilage are in a hypoxic environment under normal physiological conditions. Therefore, PEG hydrogels seeded with a high cell concentration emulate a hypoxic environment and may provide a 3D model with which to study chondrocyte mechanotransduction pathways under hypoxia.

Acknowledgments

This work was supported by the NIH with research grant from the NIDCR (K22 DE016608) and NASA Harriet Jenkins Predoctoral Fellowship and a Department of Education's Graduate Assistantship in Areas of National Need Fellowship to IV. The authors would like to thank Jeff Arthur, Mark Rice and Garret Nicodemus for their technical input.

References

1. Sah RLY, Kim YJ, Doong JYH, Grodzinsky AJ, Plaas AHK, Sandy JD. Biosynthetic response of cartilage explants to dynamic compression. J Orthop Res. 1989; 7:619–636. [PubMed: 2760736]
2. Guilak F, Ratcliffe A, Mow VC. Chondrocyte deformation and local tissue strain in articular cartilage: A confocal microscopy study. J Orthop Res. 1995; 13:410–421. [PubMed: 7602402]
3. Kim YJ, Bonassar LJ, Grodzinsky AJ. The role of cartilage streaming potential, fluid-flow and pressure in the stimulation of chondrocyte biosynthesis during dynamic compression. J Biomech. 1995; 28:1055–1066. [PubMed: 7559675]
4. Hansen U, Schunke M, Domm C, Ioannidis N, Hassenpflug J, Gehrke T, et al. Combination of reduced oxygen tension and intermittent hydrostatic pressure: a useful tool in articular cartilage tissue engineering. J Biomech. 2001; 34(7):941–949. [PubMed: 11410177]
5. Sandell LJ, Aigner T. Articular cartilage and changes in arthritis: An introduction: Cell biology of osteoarthritis. Arthritis Res. 2001; 3:107–113. [PubMed: 11178118]
6. Meachim G, Brooke G. The pathology of osteoarthritis. 1984
7. Moncada S, Higgs EA. Endogenous Nitric-oxide - physiology, pathology and clinical relevance. Eur J Clin Invest. 1991; 21(4):361–374. [PubMed: 1718757]
8. Lotz M, Hashimoto S, Kühn K. Mechanisms of chondrocyte apoptosis. Osteoarthritis Cartilage. 2002; 7(4):389–391. [PubMed: 10419776]
9. Studer RK LE, Georgescu H, Miller L, Jaffurs D, Evans CH. Nitric oxide inhibits chondrocyte response to IGF-I: inhibition of IGF-IRbeta tyrosine phosphorylation. Am J Physiol: Cell Physiol. 2000; 279(4):961–969.
10. Amin A, Abramson S. The role of nitric oxide in articular cartilage breakdown in osteoarthritis. Curr Opin Rheumatol. 1998; 10:263–268. [PubMed: 9608331]
11. Studer RK, Jaffurs D, Stefanović-Racić M, Robbins PD, Evans CH. Nitric oxide in arthritis. Osteoarthritis Cartilage. 1999; 7:377–379. [PubMed: 10419772]
12. Abramson SB, Amin AR, Clancy RM, Attur M. The role of nitric oxide in tissue destruction. Best Pract Res Clin Rheumatol. 2001; 15(5):831–845. [PubMed: 11812024]
13. Murrell GAC, Jang D, Williams RJ. Nitric-Oxide activates metalloprotease enzymes in articular-cartilage. Biochem Biophys Res Comm. 1995; 206(1):15–21. [PubMed: 7529496]
14. Sasaki K, Hattori T, Fujisawa T, Takahashi K, Inoue H, Takigawa M. Nitric oxide mediates interleukin-1-induced gene expression of matrix metalloproteinases and basic fibroblast growth factor in cultured rabbit articular chondrocytes. J Biochem. 1998; 123(3):431–439. [PubMed: 9538225]

15. Villalobo A. Nitric oxide and cell proliferation. FEBS J. 2006; 273:2329–2344. [PubMed: 16704409]
16. Blanco FJ, Lotz M. IL-1-induced nitric oxide inhibits chondrocyte proliferation via PGE2. Exp Cell Res. 1995; 218(1):319–325. [PubMed: 7537695]
17. Guerne PA, Sublet A, Lotz M. Growth factor responsiveness of human articular chondrocytes: distinct profiles in primary chondrocytes, subcultured chondrocytes, and fibroblasts. J Cell Physiol. 1994; 158(3):476–484. [PubMed: 8126071]
18. Stefanovic-Racic M, Watkins SC, Kang R, Turner D, Evans CH. Identification of inducible nitric oxide synthase in human osteoarthritic cartilage. Trans Orthop Res Soc. 1996; 21:534.
19. Matsuchita T, Fukuda K, Yamazaki K, Yamamoto N, Asada S, Yoshida K, et al. Hypoxia-induced nitric oxide protects chondrocytes from damage from hydrogen peroxide. Inflamm Res. 2004; 53:344–350. [PubMed: 15316664]
20. Das P, Schurman DJ, Smith RL. Nitric oxide and G proteins mediate the response of bovine articular chondrocytes to fluid-induced shear. J Orthop Res. 1997; 15(1):87–93. [PubMed: 9066531]
21. Hung CT, Henshaw DR, Wang CCB, Mauck RL, Raia F, Palmer G, et al. Mitogen-activated protein kinase signaling in bovine articular chondrocytes in response to fluid flow does not require calcium mobilization. J Biomech. 2000; 33(1):73–80. [PubMed: 10609520]
22. Lee DA, Bader DL. Compressive strains at physiological frequencies influence the metabolism of chondrocytes seeded in agarose. J Orthop Res. 1997; 15(2):181–188. [PubMed: 9167619]
23. Buschmann MD, Hunziker EB, Kim YJ, Grodzinsky AJ. Altered aggrecan synthesis correlates with cell and nucleus structure in statically compressed cartilage. J Cell Sci. 1996; 109:499–508. [PubMed: 8838673]
24. Bonassar LJ, Grodzinsky AJ, Frank EH, Davila SG, Bhaktav NR, Trippel SB. The effect of dynamic compression on the response of articular cartilage to insulin-like growth factor-I. J Orthop Res. 2001; 19:11–17. [PubMed: 11332605]
25. Fermor B, Weinberg JB, Pisetsky DS, Misukonis MA, Fink C, Guilak F. Induction of cyclooxygenase-2 by mechanical stress through a Nitric Oxide-regulated pathway. Osteoarthritis Cartilage. 2002; 10(10):792–798. [PubMed: 12359165]
26. Fermor B, Weinberg J, Pisetsky D, Misukonis M, Banes A, Guilak F. The effects of static and intermittent compression on nitric oxide production in articular cartilage explants. J Orthop Res. 2001; 19(4):729–737. [PubMed: 11518285]
27. Freeman PM, Natarajan JH, Kimura JH, Andriacchi TP. Chondrocyte cells respond mechanically to compressive loads. J Orthop Res. 1994; 12:311–320. [PubMed: 8207584]
28. Knight MM, Lee DA, Bader DL. Distribution of chondrocyte deformation in compressed agarose gel using confocal microscopy. Cell Eng. 1996; 1:97–102.
29. Lee DA, Knight MM, F. Bolton J, Idowu BD, Kayser MV, Bader DL. Chondrocyte deformation within compressed agarose constructs at the cellular and sub-cellular levels - evidence for the presence of stretch-activated membrane ion channel. J Biomech. 2000; 33(1):81–95. [PubMed: 10609521]
30. Lee DA, Noguchi T, Knight M, O'Donnell L, Bentley G, Bader DL. Response of chondrocyte subpopulations cultured within unloaded and loaded agarose. J Orthop Res. 1998; 16:726–733. [PubMed: 9877398]
31. Bryant SJ, Chowdhury TT, Lee DA, Bader DL, Anseth KS. Crosslinking density influences chondrocyte metabolism in dynamically loaded photocrosslinked poly(ethylene glycol) hydrogels. Ann Biomed Eng. 2004; 32(3):407–417. [PubMed: 15095815]
32. Bryant SJ, Anseth KS, Lee DA, Bader DL. Crosslinking density influences the morphology of chondrocytes photoencapsulated in PEG hydrogels during the application of compressive strain. J Orthop Res. 2004; 22:1143–1149. [PubMed: 15304291]
33. Bryant SJ, Anseth KS. Hydrogel properties influence ECM production by chondrocyte photoencapsulated in poly(ethylene glycol) hydrogels. J Biomed Mater Res. 2001; 59:63–72. [PubMed: 11745538]
34. Flory, PJ. Principles of Polymer Chemistry. Ithaca, NY: 1953.

35. Kim YJ, Sah RLY, Doong JYH, Grodzinsky AJ. Fluorometric assay of DNA in cartilage explants using Hoechst-33258. Anal Biochem. 1988; 174(1):168–176. [PubMed: 2464289]
36. Farndale RW, Buttle DJ, Barrett AJ. Improved quantitation and discrimination of sulfated glycosaminoglycans by use of dimethylmethylene blue. Biochim Biophys Acta. 1986; 883:173–177. [PubMed: 3091074]
37. Masuda K, Shirota H, Thonar EJ-MA. Quantification of 35S-labeled proteoglycans complexed to alcian blue by rapid filtration in multiwell plates. Anal Biochem. 1994; 217:167–175. [PubMed: 7515600]
38. Timmins M, Haq T. Calculating oxygen concentration from fluorescence data on the BD™ oxygen biosensor system. BD Biosciences Discovery Labware Technical Bulletin 443. 2002
39. Bryant SJ, Anseth KS. Hydrogel properties influence ECM production by chondrocytes photoencapsulated in poly(ethylene glycol) hydrogels. J Biomed Mater Res. 2002; 59(1):63–72. [PubMed: 11745538]
40. Hung CT, LeRoux MA, Palmer GD, Chao PHG, Lo S, Valhmu WB. Disparate aggrecan gene expression in chondrocytes subjected to hypotonic and hypertonic loading in 2D and 3D culture. Biorheology. 2003; 40(1–3):61–72. [PubMed: 12454388]
41. Quinn TM, Grodzinsky AJ, Buschmann MD, Kim YJ, Hunziker EB. Mechanical compression alters proteoglycan deposition and matrix deformation around individual cells in cartilage explants. J Cell Sci. 1998; 111:573–583. [PubMed: 9454731]
42. Korhonen RK, Julkunen P, Rieppo J, Lappalainen R, Konttinen YT, Jurvelin JS. Collagen network of articular cartilage modulates fluid flow and mechanical stresses in chondrocyte. Biomechan Model Mechanobiol. 2006; 5(2–3):150–159.
43. Sah RL, Kim YJ, Doong JY, Grodzinsky AJ, Plaas AH, Sandy JD. Biosynthetic response of cartilage explants to dynamic compression. J Orthop Res. 1989; 7:619–636. [PubMed: 2760736]
44. Buschmann MD, Gluzband YA, Grodzinsky AJ, Hunziker EB. Mechanical compression modulates matrix biosynthesis in chondrocyte/agarose culture. J Cell Sci. 1995; 108:1497–1508. [PubMed: 7615670]
45. Lee DA, Frean SP, Lees P, Bader DL. Dynamic mechanical compression influences nitric oxide production by articular chondrocytes seeded in agarose. Biochem Biophys Res Comm. 1998; 251:580–585. [PubMed: 9792816]
46. Lotz M. The role of nitric oxide in articular cartilage damage. Rheum Dis Clin North Am. 1999; 25(2):269–282. [PubMed: 10356417]
47. Clancy R. Nitric oxide alters chondrocyte function by disrupting cytoskeletal signaling complexes. Osteoarthritis Cartilage. 1999; 7(4):399–400. [PubMed: 10419779]
48. Matsushita T, Fukuda K, Yamazaki K, Yamamoto N, Asada S, Yoshida K, et al. Hypoxia-induced nitric oxide protects chondrocytes from damage by hydrogen peroxide. Inflamm Res. 2004; 53(8): 344–350. [PubMed: 15316664]
49. Hashimoto K, Fukuda K, Yamazaki K, Yamamoto N, Matsushita T, Hayakawa S, et al. Hypoxia-induced hyaluronan synthesis by articular chondrocytes: the role of nitric oxide. Inflamm Res. 2006; 55(2):72–77. [PubMed: 16612567]
50. Saini S, Wick TM. Effect of low oxygen tension on tissue-engineered cartilage construct development in the concentric cylinder bioreactor. Tissue Eng. 2004; 10:825–832. [PubMed: 15265300]
51. Heywood H, Lee DA, Bader DL. Rate of oxygen consumption by isolated articular chondrocytes is sensitive to medium glucose concentration. J Cell Physiol. 2006; 206:402–410. [PubMed: 16155906]

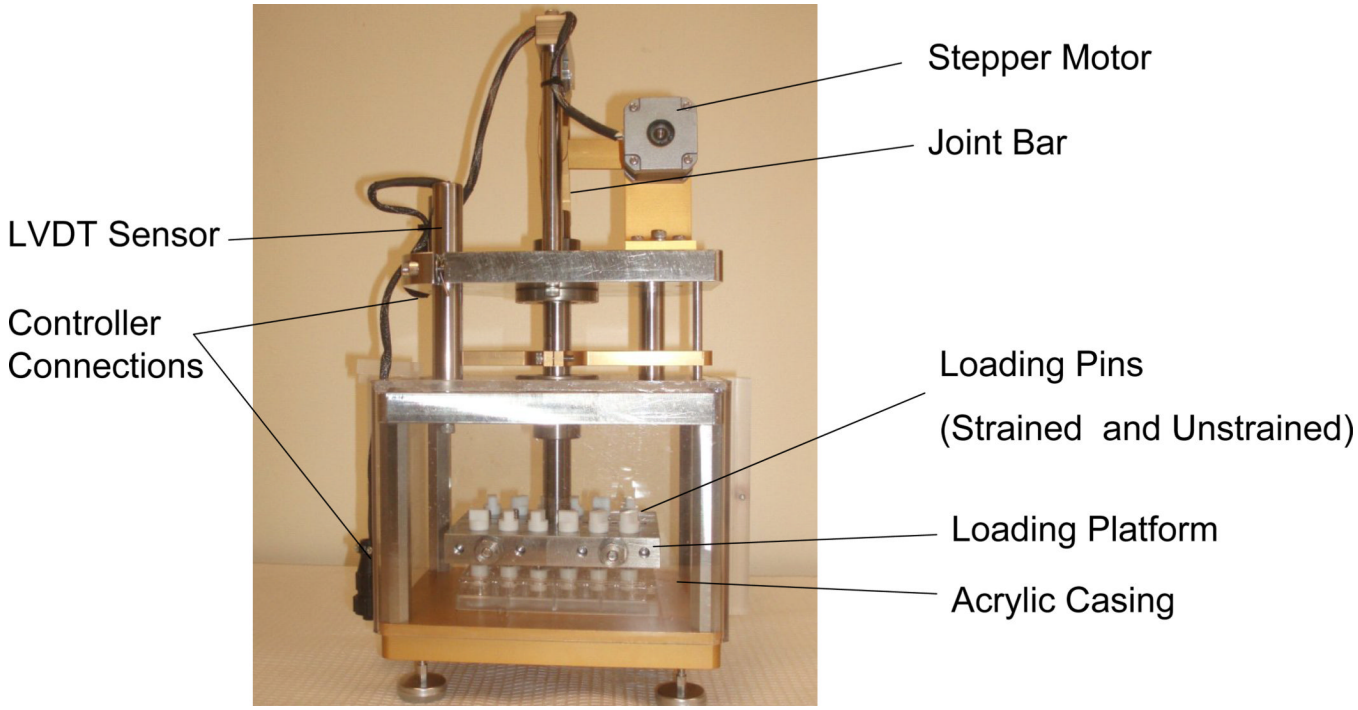

Figure 1.
Custom designed loading apparatus. The loading mechanism consists of a rod-linkage assembly controlled by a stepper motor. The loading chamber contains 24 non-porous loading platens that are associated with each well of a standard 24 well plate.

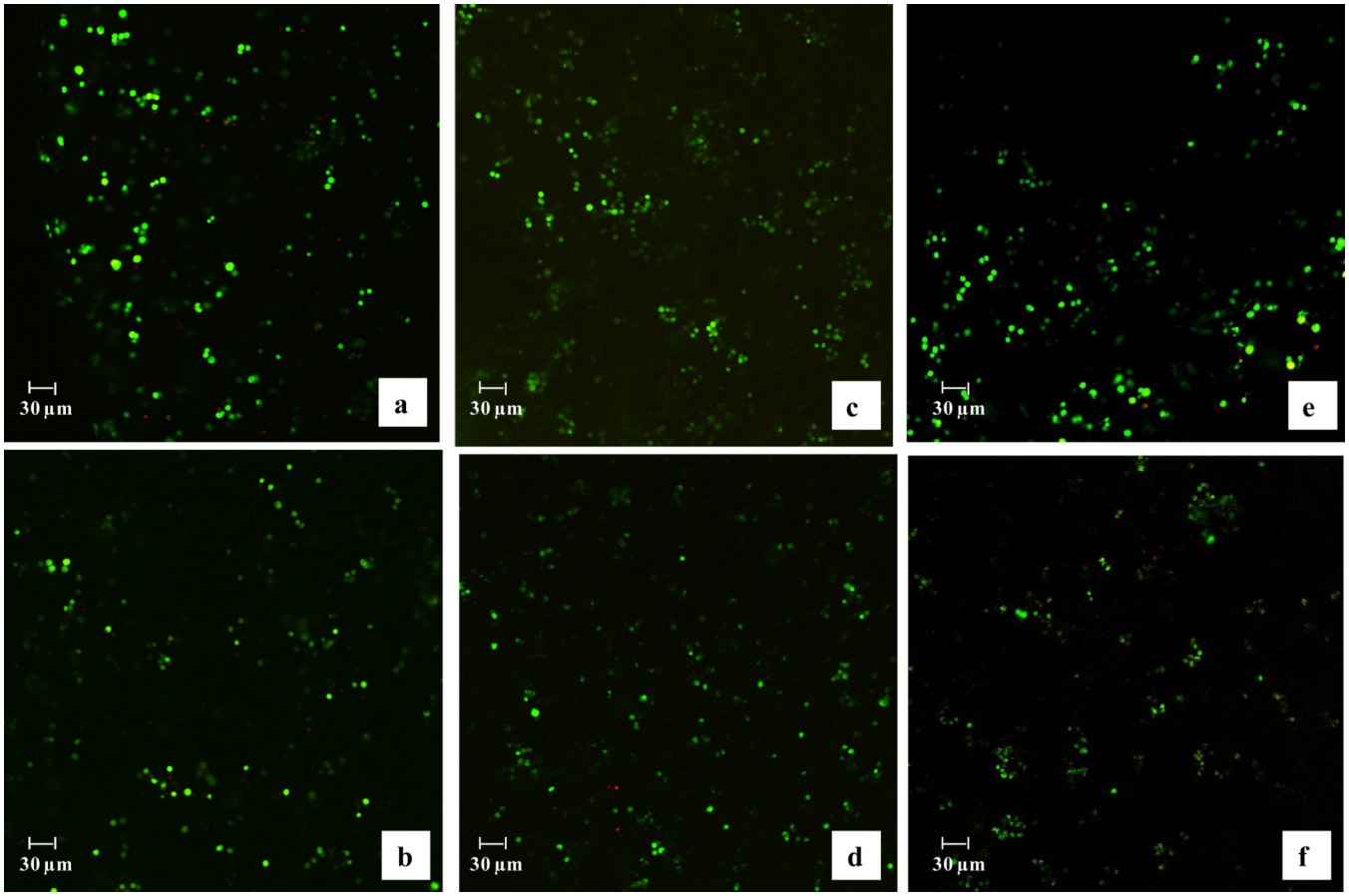

Figure 2.
Chondrocytes encapsulated in PEG hydrogels with low (a,b), medium (c,d) and high (e,f) crosslinking and cultured as unstrained controls (a,c,e) or subjected to dynamic loading conditions at 1.0 Hz for 48 hours (b,d,f). Live cells = green, dead cells = red. Similar viabilities were observed with static loading and 0.3 Hz loading frequencies. The original image dimensions are 225 µm × 225 µm with a magnification of 10×.

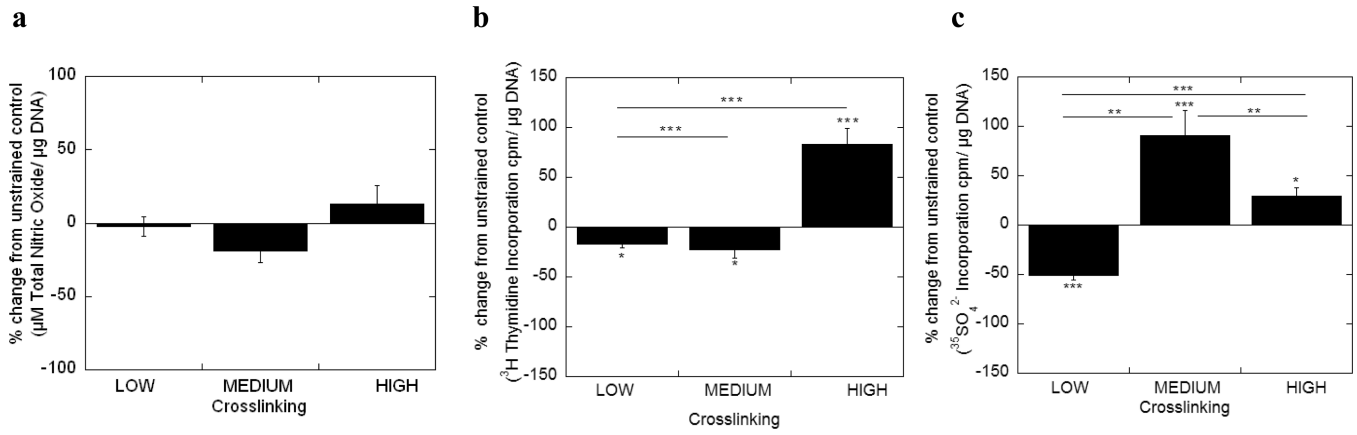

Figure 3.

Total nitric oxide production (a), cell proliferation (b) and proteoglycan synthesis (c) by chondrocytes encapsulated in low, medium and high crosslinked hydrogels subjected to 15% static strains for 48 hours. Cell response was normalized to the unstrained control as a percent change. Data is given by mean ± standard error of mean (n=8); *p<0.05, **p<0.01, ***p<0.001. An asterisk(s) above a column denotes significance from control.

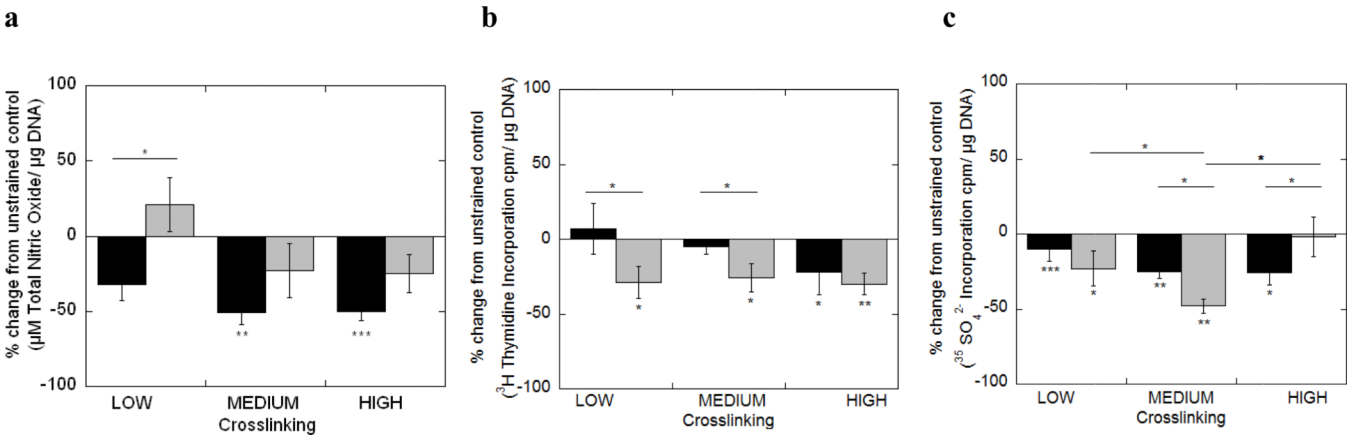

Figure 4.

Total nitric oxide production (a), cell proliferation (b) and proteoglycan synthesis (c) by chondrocytes encapsulated in low, medium and high crosslinked hydrogels subjected to dynamic strains at 0.3 Hz (black bars) or 1 Hz (gray bars) with 15% amplitude strains for 48 hours. Cell response was normalized to the unstrained control as a percent change. Data is given by mean ± standard error of mean (n=8); *p<0.05, **p<0.01, ***p<0.001. An asterisk(s) above a column denotes significance from control.

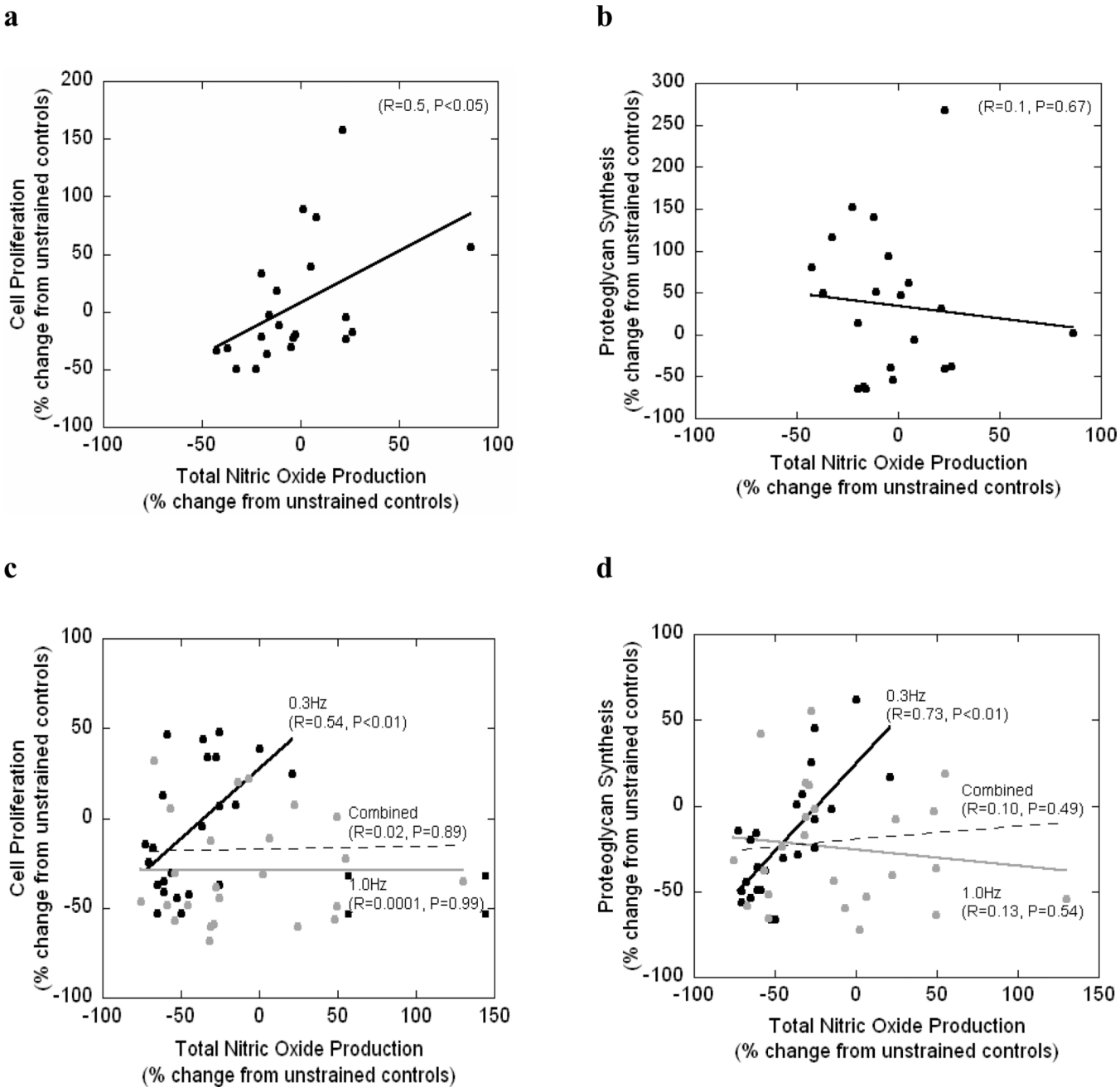

Figure 5.

Regression analysis for cell proliferation as a function of total NO production (a,c) or proteoglycan synthesis as a function of total NO production (b,d) for statically strained PEG constructs (a,b) and dynamically strained PEG constructs (c,d). For panel c and d, regression analysis was performed for 0.3Hz dynamically strained gels (black circles, black line) and for the 1.0Hz dynamically strained gels (gray circles, gray line) and for both frequencies combined (dotted line).

Table 1

PEG hydrogel properties*

Crosslinking	PEGDM (%)†	ρ_x (mol/L) ‡	Q§	K (kPa) //	E* (kPa) ¶	
					0.3Hz	1.0Hz
LOW	10	0.110 ± 0.001	12.2 ± 1.1	60 ± 5	70 ± 2	100 ± 4
MEDIUM	20	0.410 ± 0.070	5.5 ± 1.0	500 ± 14	800 ± 38	1200 ± 11
HIGH	**30**	0.650 ± 0.067	4.7 ± 0.5	900 ± 54	1200 ± 76	1400 ± 49

*data reported as mean ± standard deviation;

†percent poly(ethylene glycol) dimethacrylate macromer in solution prior to polymerization;

‡crosslinking density;

§equilibrium volumetric swelling ratio;

//tangent compressive modulus;

¶dynamic compressive modulus.

Table 2

Chondrocyte viability in unstrained and strained PEG gels *

Crosslinking	Unstrained	Static	Dynamic	
			0.3 Hz	1 Hz
LOW	79 ± 3%	77 ± 9%	73 ± 7%	76 ± 2%
MEDIUM	76 ± 4.4%	76 ± 6%	85 ± 8%	78 ± 2%
HIGH	77 ± 5.3%	76 ± 7%	76 ± 6%	78 ± 0.9%

* data reported as mean ± standard deviation.

Table 3

Chondrocyte diameters and diameter ratios in unstrained and strained PEG gels*

Crosslinking	Unstrained			Strained†		
	Cell diameter (μm)		Diameter Ratio	Cell diameter (μm)		Diameter Ratio
	X	Y	(X/Y)	X	Y	(X/Y)
LOW	11.67 ± 0.45	11.90 ± 0.46	0.98 ± 0.05	10.42 ± 0.03§	13.20 ± 0.13§	0.79 ± 0.01‡
MEDIUM	11.63 ± 0.12	11.91 ± 0.39	0.98 ± 0.03	10.28 ± 0.06¶	13.50 ± 0.09¶	0.76 ± 0.01// §§
HIGH	11.70 ± 0.36	12.04 ± 0.24	0.97 ± 0.04	10.06 ± 0.02‡‡	13.84 ± 0.17‡‡	0.73 ± 0.01**, §§,///

*data reported as mean ± standard error of mean;

†total applied strain for low (19.8%), medium (15.7%) and high (15.5%) crosslinked gels;

‡p<0.05 compared to the low crosslinking density without strain;

§p<0.001 compared to the low crosslinking density without strain;

//p<0.01compared to the medium crosslinking density without strain;

¶p<0.001 compared to the medium crosslinking density without strain;

**p<0.01 compared to the high crosslinking density without strain;

‡‡p<0.001 compared to the high crosslinking density without strain;

§§p<0.05 compared to the low crosslinking density with strain;

///p<0.05 compared to the medium crosslinking density with strain.

Table 4

Statistical analysis for statically strained PEG hydrogels*

Factor	Measure	SS†	MS ‡	Var§	P-value
Crosslinking	Total NO Production	3521	1760	2.5	>0.05
	Cell Proliferation	35577	17786	15.2	<0.001
	Proteoglycan Synthesis	114054	57027	29.6	<0.001

*Anova for two factor fixed effects model; SS=Sum of Squares; MS=Mean Square; Var=Variance.

Table 5

Statistical analysis for dynamically strained PEG hydrogels*

Factor	Measure	SS	MS	Var	P-value
Crosslinking	Total NO Production	15490	7745	12.03	<0.001
	Cell Proliferation	3193	1597	2.10	>0.05
	Proteoglycan Synthesis	6544	3272	5.62	<0.001
Loading Frequency	Total NO Production	14651	14651	22.75	<0.001
	Cell Proliferation	5833	5833	7.67	<0.01
	Proteoglycan Synthesis	186	186	0.32	>0.05
Interaction	Total NO Production	27671	13836	21.49	<0.001
	Cell Proliferation	13016	6508	8.55	<0.001
	Proteoglycan Synthesis	24027	12013	20.65	<0.001

*Anova for two factor fixed effects model; SS=Sum of Squares; MS=Mean Square; Var=Variance.

Osteoarthritis Cartilage. Author manuscript; available in PMC 2012 March 20.

Table 6

Oxygen consumption in PEG gels*

O_2 Concentration (μM)		
Crosslinking	**0 hr**	**48 hr**
LOW	164 ± 7	20 ± 10†
MEDIUM	164 ± 7	20 ± 8†
HIGH	164 ± 7	23 ± 9†

* data reported as mean ± standard deviation.

† $p<0.001$ compared to 0 hours of its respective crosslinked gel.